Available online at www.sciencedirect.com

SciVerse ScienceDirect

Journal of the European Ceramic Society 32 (2012) 1519–1528

www.elsevier.com/locate/jeurceramsoc

# Extended studies of degradation mechanisms in the refractory lining of a rotary kiln for iron ore pellet production

Jesper Stjernberg [a,*], John C. Ion [a], Marta-Lena Antti [a], Lars-Olof Nordin [b], Bo Lindblom [b], Magnus Odén [c]

[a] *Division of Materials Science, Luleå University of Technology, 971 87 Luleå, Sweden*
[b] *LKAB, 971 28 Luleå, Sweden*
[c] *Nanostructured Materials, Dept. Physics, Linköping University, 581 83 Linköping, Sweden*

Received 4 October 2011; received in revised form 29 December 2011; accepted 7 January 2012
Available online 2 February 2012

**Abstract**

Changes, over a period of 8 years, in the chemical composition and morphology of deposit and lining materials in a production rotary kiln for iron ore pellet manufacture are described. The following have been studied: two types of refractory brick used as lining material; deposited chunk materials from the lining; the interaction zones between deposits and linings. Morphological changes at the deposit/lining interface, and the active chemical reactions, are established. Larger hematite grains in the deposit material (5–50 μm) primarily remain at the original deposit/lining interface. The remainder penetrates fissures, voids and brick joints, forms a laminar structure with corundum from the bricks, and migrates in grains in the lining material. Potassium penetrates more deeply into the bricks than hematite, resulting in the formation of kalsilite, leucite and potassium β-alumina, which contribute to degradation of the lining.


*Keywords:* B. Electron microscopy; C. Corrosion; D. $Al_2O_3$; D. Mullite; E. Refractories

## 1. Introduction

The pelletising of iron ore as a burden material for blast furnaces has been used commercially since the early 1950s. Two main processes are used today during such production: the travelling grate and the grate-kiln process.[1] In the grate-kiln process, which is studied here, the grate is a pre-heater and the kiln is a rotating furnace lined with refractory bricks. The refractory lining degrades over time through exposure to high temperatures and a corrosive environment, requiring replacement at regular intervals. Degradation mechanisms in rotary kilns are complex since several different mechanisms operate simultaneously. The main source of degradation is residue from pellet production which together with fly ash from coal burned to heat the kiln, forms deposits on the lining that accumulate in chunks.[2] Fig. 1 shows such deposits in the kiln studied in this work (KK2, Loussavaara Kiirunavaara Limited (LKAB), Kiruna, Sweden), observed during a production stop. Adhesion of deposits on the refractories has also been observed at other iron ore pellet production sites and in different types of kiln; which appears to be related to the quality and composition of the burner fuel used.[3]

The formation and location of the deposits in the kiln varies, but in general, there is more deposition of material in the warmer zone closest to the burner. The deposition can reach a thickness up to 30 cm; with peaks protruding like stalactites, with lengths up to 1 m. However, some zones in the kiln can be without any deposition. A thin layer of deposition is considered protective, as it insulates and lowers the liner temperature, and is protective against wear. When this layer grows too thick, mechanical action occasionally causes fallout of heavy chunk formations that can cause exfoliation of the lining, creating a new hot face where pellet residues and fly ash once again come into contact with fresh lining material, and are able to deposit in chunks.

The kiln studied here rotates clockwise (observed from the outlet) at approx. 2 rpm, and is tilted 3° to the horizontal plane such that the pellets travel more easily towards its outlet, through a helical movement. Fig. 2 shows the design of the kiln. It has a length of 33.2 m, and an inner diameter of 5.64 m at the inlet

* Corresponding author. Tel.: +46 920 224705.
*E-mail address:* jessje@ltu.se (J. Stjernberg).

0955-2219/$ – see front matter © 2012 Elsevier Ltd. All rights reserved.
doi:10.1016/j.jeurceramsoc.2012.01.012

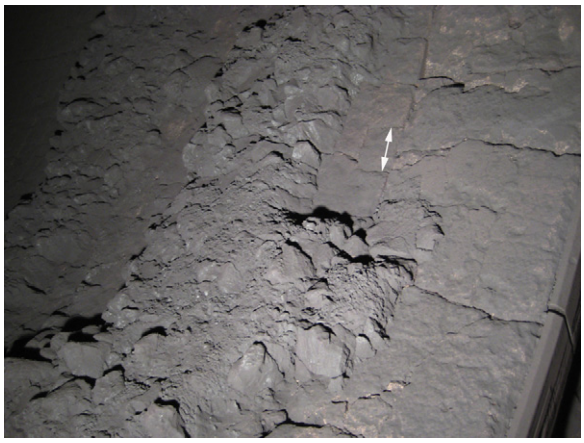

Fig. 1. Photo showing deposits in the kiln KK2, Kiruna, Sweden, June 2010. The white arrow in the image marks the brick width, which is 17.5 cm.

(where the feed enters) and 5.04 m at the outlet (dimensions in the drawing are the outer diameter of the refractories at the steel shell). A burner is located at the outlet of the kiln. It is primarily fuelled with coal, but oil is used at start-ups and if problems in the feed of coal arise. The length of the flame and the location of the hot spot formed vary with the fuel used. This can cause thermomechanical tensile stresses in the lining, resulting in thermally induced lining spallation.[4] A scheduled production stop of the kiln takes place once a year, to remove deposits and replace depleted refractory bricks. The removal of these deposits causes abrasive wear that also degrades the lining.

The temperatures at the hot face of the lining are estimated to be: at the outlet ∼1250 °C; at the burner zone where the flame heats the most (around 10–15 m from the outlet, varies with fuel and operative conditions) ∼1350 °C; and at the inlet ∼1200 °C. However, these numbers are often only valid at start-ups of the plant. As soon as material adheres to the surface, the surface-lining temperature might be lowered several hundreds of degrees, as deposits act to protect against heat.

The two types of refractory brick used in the kiln studied are made from a basis of chamotte (installed in the first third of the kiln where lower temperatures are encountered) and bauxite (in the remainder of the kiln where temperatures may exceed 1400 °C). Mullite ($3Al_2O_3{\cdot}2SiO_2$) and corundum ($Al_2O_3$) are formed during manufacture of the bricks. The chemical composition in the bricks varies slightly between production batches, resulting in variations in the phases that form during service. It can therefore be difficult to compare as-fabricated bricks with bricks that have been in use for some time. However, by knowing the approximate chemical compositions of the bricks and the deposit material, the phases and minerals associated with the original liner can be distinguished from those that evolve during use.

The dominant constituents in both types of brick are alumina ($Al_2O_3$) and silica ($SiO_2$), with traces of other oxides. $Al_2O_3$ and $SiO_2$, present in a ratio of 3:2, form the mineral mullite during heat treatment, which has appropriate refractory properties, i.e. a high melting temperature, low thermal expansion coefficient and low thermal conductivity. Mullite is a solid solution described stoichiometrically as $Al_{4+2x}Si_{2-2x}O_{10-x}$, where $x$ is the number of oxygen vacancies which varies between 0.2 and 0.9. However, mullite is more commonly expressed stoichiometrically by the oxide formula $3Al_2O_3{\cdot}2SiO_2$.[5] In addition to these oxides, $TiO_2$ and CaO are present in lower concentrations in both types of brick – these oxides are commonly found as constituents in refractory materials. Traces of $Fe_2O_3$, $K_2O$ and $Na_2O$ are also present – these accessory oxides were previously considered unimportant, but are now recognised to be controlling factors in the performance of lining materials.[6] In addition to chemical composition, factors such as grain size and porosity affect the properties and behaviour of a lining material during use.

Laboratory scale studies of this refractory-deposit system,[7,8] indicated that the liners are strongly affected by the presence of alkalis. However, detailed descriptions of the deterioration mechanisms acting on the lining of a production kiln are still not available. An improved understanding of these could help to increase lifetime through selection of correct brick composition. The objective of this paper is to provide detailed descriptions of the reactions occurring at the interface between the bricks and deposits, based on samples collected from a production kiln.

## 2. Materials

Table 1 gives the chemical analyses of the bricks used in this kiln, in terms of the most stable oxides. During manufacturing of the bricks, mullite and corundum are mainly formed. However, the bricks also contains traces of other oxides e.g. cristobalite and quartz. Both types of brick were produced by Höganäs Bjuf AB (Bjuv, Sweden).

Samples of bricks that had served as refractory liners in a production kiln, which had deposits adhered to their surfaces, were collected at different locations in an LKAB production kiln (KK2), during two production stops, 2 years apart (June 2008 and June 2010).

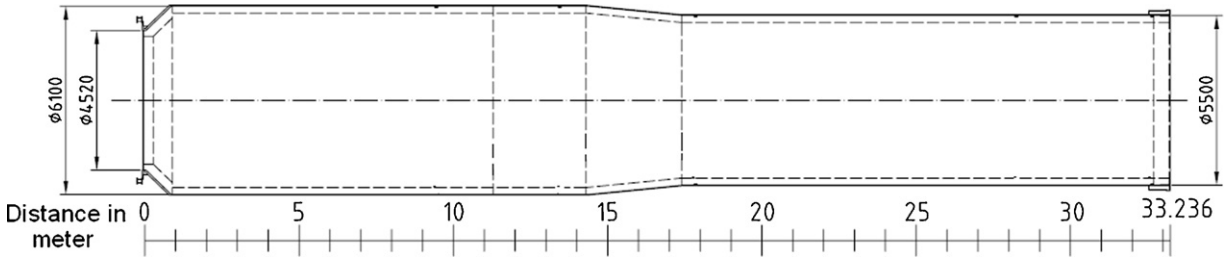


Fig. 2. Schematic diagram of the KK2 kiln located in Kiruna, Sweden.

Table 1
Nominal chemical compositions (wt%) of two commercial bricks (manufacturer's data).

| | Bauxite based brick | Chamotte based brick |
|---|---|---|
| $Al_2O_3$ | ∼73 | ∼58 |
| $SiO_2$ | ∼26 | ∼36 |
| CaO | 0.2 | 0.3 |
| $TiO_2$ | 2.7 | 2.1 |
| $Fe_2O_3$ | 1.1 | 1.4 |
| Alkalis | 0.3 | 1.3 |

Deposits were also collected from an industrial kiln during two production stops, 4 years apart (May 2006 and June 2010). Table 2 gives an overview of the samples and analysis methods used in the present study.

## 3. Analysis techniques

The chemical compositions of the deposit materials were determined by X-ray fluorescence spectroscopy (XRF) using a PANalytical MagiX instrument (software, SuperQ), calibrated with certified references. The materials tested were first transformed to fused beads by a Herzog HAG 12 inductive fusion machine. Analyses were carried out using rhodium X-ray radiation with flow proportional counters for Na, Mg and Al and a scintillation counter for all other elements over a $2\theta$ interval between 22° and 145°. The different valance states of iron ($Fe^{2+}$ and $Fe^{3+}$) were differentiated using a titration method with potassium dichromate (ISO 9035).

X-ray diffractometry (XRD) was carried out using a Philips X-ray diffractometer (MRD) using Cu Kα radiation. The diffractograms were recorded over a $2\theta$ interval between 10° and 90°. Refractory brick material collected from the production kiln, as well as refractory brick material in the as-fabricated condition, were studied. Adhered deposit materials were removed from the brick liners and the liner material closest to the surfaces (within 1 cm of the lining/deposit interface) and milled to powders prior to analysis. These samples were compared with as-fabricated bricks of similar quality, which were also milled to powders.

The interaction zones between the deposits and the liners were studied using optical and electron microscopy. Selected interfaces were polished and carbon coated prior to microscopy. Scanning electron microscopy (SEM) studies were performed using a JEOL JSM-6460 microscope (INCA software) equipped with an energy dispersive spectrometer (EDS). All the SEM micrographs shown were recorded in the back scattered mode, except EDS mappings. Optical microscopy (OM) studies were performed using a Moritex MS-500C.

## 4. Results

### 4.1. Deposit materials

Table 3 shows the chemical composition of the deposit material collected at different locations in the kiln studied, on two occasions 4 years apart. On both occasions, the deposition had a year of build up since the last production stop. In all samples collected, the deposited material was dominated by iron oxides, mainly $Fe_2O_3$ (hematite), in concentrations around 95 wt% along the entire length of the kiln. In 2006, $K_2O$ and $Na_2O$ were found in comparable concentrations along the kiln length; however, the concentrations of $Na_2O$ are below the detection limit in all samples collected in 2010. The oxides MgO, MnO, $TiO_2$, $P_2O_5$ and $V_2O_5$ all appear in stable concentrations over time and along the length of the kiln. The concentrations of sulphur, CaO, $Al_2O_3$ and $SiO_2$ vary irregularly along the length of the kiln.

### 4.2. Bauxite based bricks

#### 4.2.1. After 14 months in service

Fig. 3(a) and (b) shows the lining–deposit interface in a sample collected 6 m from the outlet of the kiln, where the bauxite based bricks have served as liners for 14 months. Cracks parallel to the hot face were observed at this location. In all the cracks examined some hematite from the deposit material remained on the lining material as the deposits flaked off, i.e. the deposit failed cohesively. The hematite dominated deposits seen in the top of Fig. 3(a) (white grains, marked H) remain on the brick surface in a distinct front. At some locations they form a laminar structure with alumina from the brick (corundum grains marked C), shown with a higher magnification in Fig. 3(b). The white lamellae comprised iron oxide with ∼1 wt% of aluminium and ∼3 wt% of titanium, while the dark lamellae comprised aluminium oxide with ∼1 wt% each of potassium and silicon. Very little glassy bonding phase exists around the corundum grains in the lining material.

Diffractograms obtained from a brick sample collected at this location (not shown) show no evidence of the formation of new phases with high enough concentrations to be detected with XRD, compared with an as-fabricated brick. A majority of the

Table 2
Overview of when samples were collected, their locations, and how they were analysed.

| Date | Service time of liners (months) | Sample type | Location (distance to outlet [m]) | Analyses performed |
|---|---|---|---|---|
| May 2006 | | Deposit | 0, 10, 20 | XRF |
| June 2008 | 48 | Brick | 30 | XRD |
| June 2008 | 48, 72 | Brick/deposit | 0, 30 | SEM |
| June 2010 | | Deposit | 0,[a] 6, 12, 25, 33 | XRF |
| June 2010 | 14, 72, 96 | Brick | 6, 12, 25 | XRD |
| June 2010 | 14, 72, 96 | Brick/deposit | 6, 12, 25 | SEM, OM |

[a] Fig. 1 was obtained at this location on this occasion.

Table 3
Chemical compositions (wt%) of the deposit materials collected in the production kiln.

| Collection year | 2006 | 2006 | 2006 | 2010 | 2010 | 2010 | 2010 | 2010 |
|---|---|---|---|---|---|---|---|---|
| Distance to outlet (m) | 0 | 10 | 20 | 0 | 6 | 12 | 25 | 33 |
| $Fe_2O_3$ | 90.31 | 91.55 | 88.27 | 94.42 | 96.66 | 94.83 | 90.18 | 92.49 |
| $Fe_3O_4$ | 2.22 | 2.22 | 2.35 | 0.94 | 0.76 | 1.05 | 3.11 | 1.41 |
| $SiO_2$ | 2.93 | 2.11 | 3.89 | 2.60 | 1.18 | 2.15 | 3.31 | 3.28 |
| $Al_2O_3$ | 0.55 | 0.54 | 1.09 | 0.46 | 0.20 | 0.44 | 0.82 | 0.83 |
| CaO | 0.52 | 0.37 | 0.55 | 0.45 | 0.23 | 0.36 | 1.31 | 0.75 |
| MgO | 0.54 | 0.48 | 0.63 | 0.51 | 0.52 | 0.58 | 0.54 | 0.55 |
| $Na_2O$ | 0.138 | 0.100 | 0.202 | <0.050 | <0.050 | <0.050 | <0.050 | <0.050 |
| $K_2O$ | 0.088 | 0.072 | 0.153 | 0.092 | 0.028 | 0.071 | 0.102 | 0.097 |
| MnO | 0.07 | 0.07 | 0.07 | 0.08 | 0.08 | 0.08 | 0.10 | 0.08 |
| $TiO_2$ | 0.21 | 0.17 | 0.20 | 0.19 | 0.18 | 0.19 | 0.19 | 0.20 |
| $V_2O_5$ | 0.19 | 0.18 | 0.17 | 0.190 | 0.130 | 0.180 | 0.170 | 0.190 |
| $P_2O_5$ | 0.060 | 0.046 | 0.071 | 0.060 | 0.023 | 0.046 | 0.073 | 0.073 |
| Total oxides | 97.83 | 97.91 | 98.38 | 97.09 | 97.02 | 97.07 | 97.46 | 97.44 |
| Sulphur | 0.0015 | 0.076 | 0.0121 | 0.0127 | 0.0266 | <0.0010 | 0.0021 | 0.0034 |

confirmed peaks correspond to corundum and mullite, including traces of andalusite ($Al_2O_3 \cdot SiO_2$) and cristobalite ($SiO_2$).

### 4.2.2. After 4 years in service

Fig. 4 shows the lining–deposit interface in a sample collected from the outlet of the kiln (to the right in Fig. 1), where bauxite based bricks have served as liners for 4 years. The hematite dominated deposit material is seen at the top of the micrograph (white grains marked H) forming a distinct interface with the remaining brick. The white arrows in Fig. 4 mark a crack approximately parallel to the lining–deposit interface. Grains of mullite are marked M, corundum is marked C. (This convention is used hereafter.)

Fig. 5(a) and (b) are enlargements of the areas marked with black and white frames in Fig. 4. Dislodged corundum grains (the dark grains in Fig. 5(a)), are released by erosion when the grain boundaries become corroded in the lining, and migrate into the deposit material surrounded by hematite grains. Note also the needles of hematite formed closest to the surface inside the corundum grain (marked with white arrows in Fig. 5(a)). Hematite and corundum are isomorphous, and have been observed to form a solid solution at elevated temperatures.[8,9] The finer interlocked mullite structure (marked I in Fig. 5(b)) loses its interlocking as it transforms to rod-like crystals (marked II in Fig. 5(b)), around the mullite aggregates. This is also observed around all other mullite aggregates at this location. White spots in the micrograph are regions of high titanium concentration.

Fig. 6(a) shows part of the sample shown in Fig. 4. Elemental EDS maps of aluminium, silicon, iron, sodium and potassium

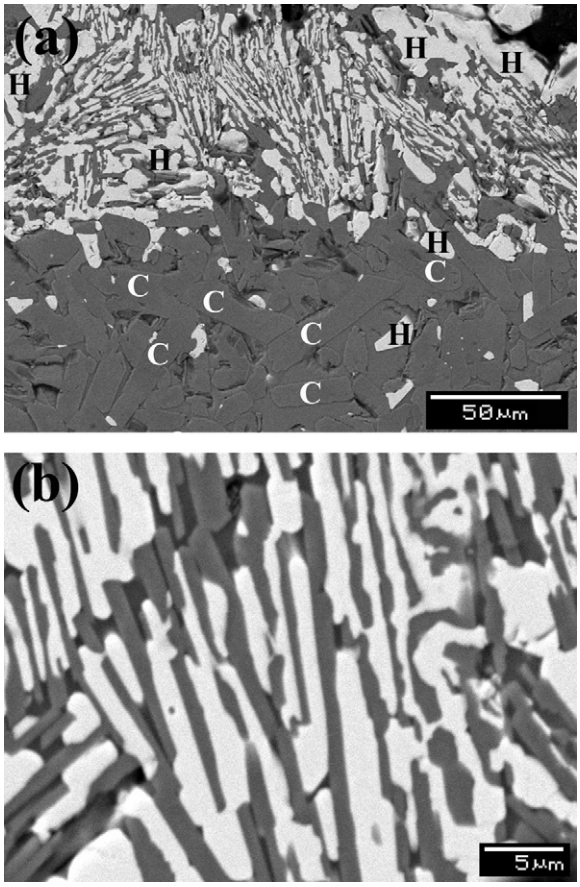


Fig. 3. SEM micrographs showing (a) a lining–deposit interface sample, collected 6 m from the outlet of the kiln, June 2010, and (b) a part of the deposit material in (a) with a higher magnification. H = hematite, C = corundum.

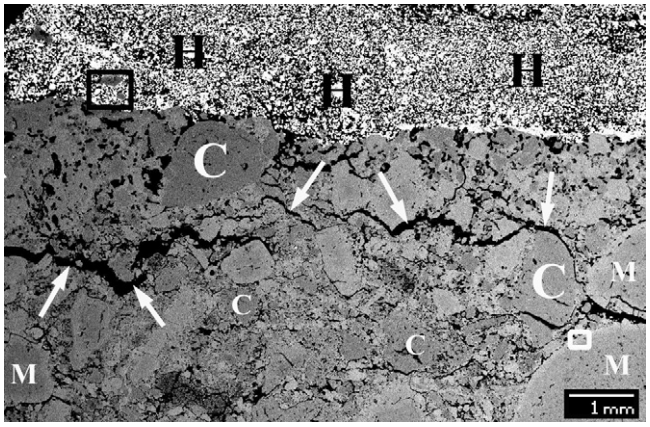


Fig. 4. SEM micrograph showing an overview of the interaction zone between deposit and lining, of a sample collected in the outlet of the kiln, June 2008. Arrows mark cracks in the lining. H = hematite, C = corundum, M = mullite.

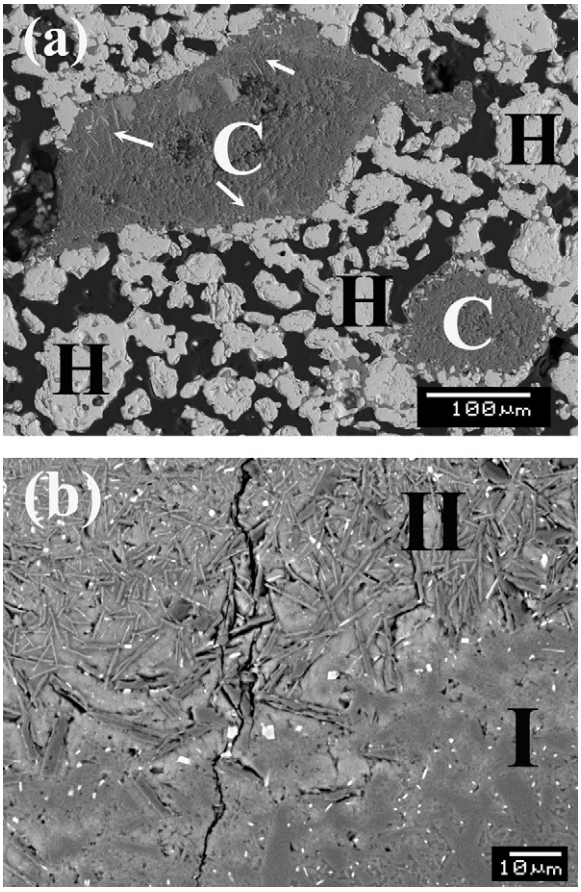


Fig. 5. SEM micrographs, showing (a) dislodged corundum grains (dark grains) migrated through the deposit material, and (b) mullite aggregate transformed in contact with potassium. Note the difference in magnification in the images. H = hematite, C = corundum, I = primary mullite, II = secondary mullite.

from the same area are shown in Fig. 6(b)–(f). Iron is seen to remain on the original lining surface. Potassium however, has migrated deep into the lining, and reacted primarily with mullite, while the reaction with corundum is more moderate. Very little sodium is detected into the lining material, compared with potassium.

#### 4.2.3. After 6 years in service

Fig. 7(a) and (b) shows the deposit–lining interface in a sample collected 12 m from the outlet of the kiln, where the bauxite based bricks have served as liners for 6 years. These two samples of the same quality, collected at the same time and location in the kiln, exhibited different properties. In Fig. 7(a), the hematite dominated deposit material seen in the top of the micrograph remains on the brick surface in a distinct front. The grains of hematite in the deposit material have sintered, and increased the particle-to-particle contact area, which results in grain growth and a more homogenous layer of hematite. Titanium oxide is observed as small white grains in the lining. However, a zone of ~100 μm closest to the deposit material (marked with a white arrow) is depleted in titanium oxide. In Fig. 7(b) however, migration of hematite grains through the lining material is seen. The corundum grains are embedded in a more glassy grain boundary phase in Fig. 7(a), compared with Fig. 7(b).

Diffractograms obtained from a brick sample collected at this location (not shown) gave similar results to those for the sample that had been in service for 14 months i.e. no new phases had formed.

### 4.3. Chamotte based bricks

#### 4.3.1. After 6 years in service

Fig. 8 shows the deposit–lining interface in a sample collected 30 m from the outlet (3 m from inlet) of the kiln, where the chamotte based bricks have served as liners for 6 years. Deposit material, dominated by hematite (white grains), is seen in the top of the micrograph. Hematite grains 5–50 μm in diameter remained on the lining surface in a distinct front. Corundum grains were detected in the lining material, together with some rod-like formations. A zone in which grains from the brick mixed with hematite grains form a denser layer (~30 μm thick) than the more porous deposit material above.

Fig. 9(a) and (b) shows XRD diffractograms recorded from a sample collected at this location, compared with that recorded from an as-fabricated brick of similar quality. In Fig. 9(a) a majority of confirmed peaks correspond to corundum and mullite, including traces of cristobalite and quartz (both $SiO_2$). In Fig. 9(b) mullite is seen to be almost depleted to an undetectable level, as is $SiO_2$. Instead, new phases have formed, notably leucite ($K_2O{\cdot}Al_2O_3{\cdot}4SiO_2$). Minor peaks in the diffractogram correspond to potassium β-alumina ($K_2O{\cdot}11Al_2O_3$) and kalsilite ($K_2O{\cdot}Al_2O_3{\cdot}2SiO_2$); these are phases detected in the sample but in concentrations less prominent than leucite and corundum.

#### 4.3.2. After 8 years in service

Fig. 10(a)–(d) shows the deposit–lining interface in samples collected 25 m from the outlet of the kiln, where the chamotte based bricks have served as liners for 8 years. Hematite is the dominant phase in the deposit material (dark in the OM micrograph and white in SEM micrographs). Fig. 10(a) shows how material from the deposits has penetrated fissures (arrow to left in the micrograph) and joints (arrow to right in the micrograph). Hematite filled joints are 400–800 μm broad while hematite filled fissures are 100–200 μm in width. Fig. 10(b) shows how the grains of hematite have started to sinter, resulting in grain growth and a more homogenous layer of hematite at the interface (marked with arrows). Clusters of hematite, which have migrated through the lining, are formed deeper in the lining. These clusters give the lining a reddish colour, Fig. 10(a). The material in the bonding phase between the hematite grains that migrated through fissures and joints appears to be of a non-crystalline morphology (Fig. 10(c) and (d)). This bonding phase exhibits high concentrations of potassium (above 10 wt%) and sodium (~3 wt%), with traces of sulphur and phosphorus.

Diffractograms obtained from a brick sample collected at this location (not shown) indicated that no new phases had formed compared with as-fabricated brick. A majority of confirmed peaks correspond to corundum and mullite, including traces of cristobalite and quartz (both $SiO_2$).

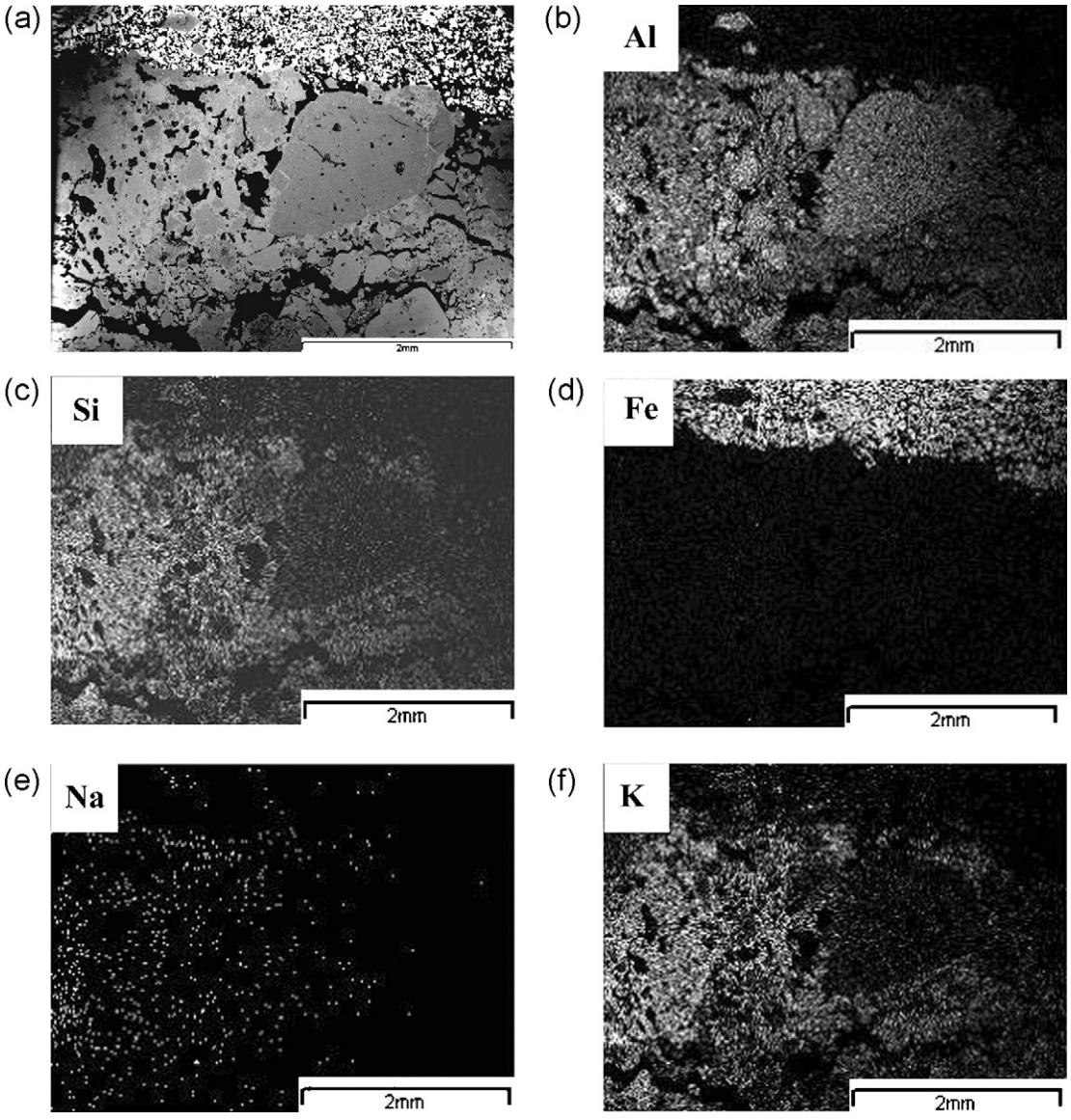


Fig. 6. (a) Back scattered SEM micrograph of parts of Fig. 4, and (b) Al, (c) Si, (d) Fe, (e) Na, (f) K shows EDS mappings of the corresponding area.

## 5. Discussion

This paper deals with different degradation mechanisms acting on the bricks serving as refractory liners in rotary kilns at iron ore pellet production. The discussion is presented in terms of the mechanisms operating.

### 5.1. Effect of potassium on the microstructure of the lining

The effect of potassium on mullite aggregates in the lining is to cause the aggregates to lose their interlocking form: the mullite transforms to needle-like formations in the lining (seen in Fig. 5(b)). These structures are also observed by Iqbal and Lee,[10–12] where primary mullite was produced from clays. They observed nucleation of primary mullite, with sizes less than 0.5 μm, while the alumina-richer secondary mullite started to grow from the primary mullite, in needle shaped formations with lengths greater than 1 μm, in the presence of an amorphous alkali-aluminosilicate melt. Schüller[13] observed that such formations of needle-like secondary mullite were affected by the presence of potash feldspar and silica, and in contrast to this, soda feldspar caused the same action at higher temperatures.

The migrated alkali metal (i.e. potassium) reacts with the mullite and binds to the acid silicon dioxide, which is released from the mullite into the glassy phase. Together, they increase the bulk volume of this phase, so that the larger secondary mullite grains, richer in alumina, become more mobile. We propose that this formation of secondary mullite, caused by the presence of potassium that occurs around the aggregates of primary mullite in the refractories studied, is a corrosive mechanism that finally promotes the degradation of the lining.

The effect of potassium penetration into the lining is that new phases form by reaction with the refractory material. Through penetration into voids, fissures and brick joints, and by diffusion along the grain boundaries, the potassium infiltrates the lining in high concentrations – at some locations to a depth of several

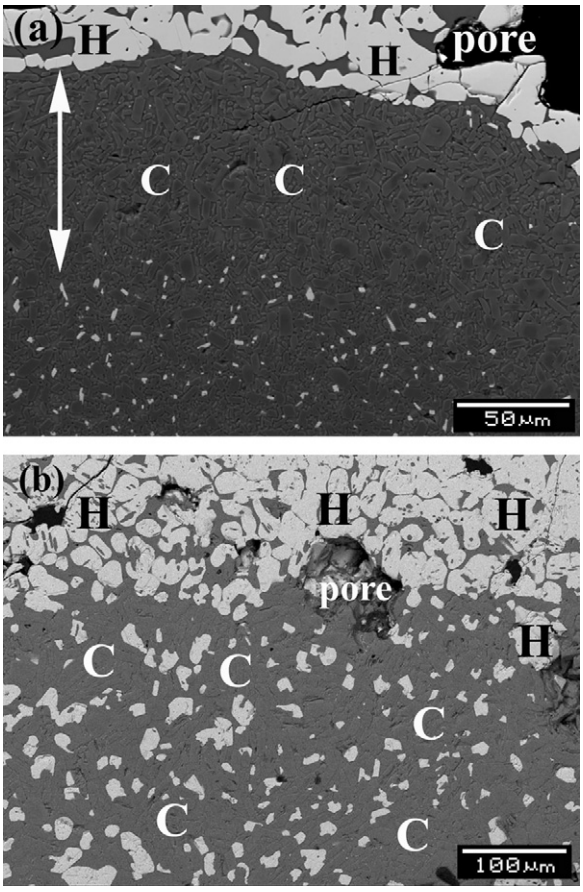


Fig. 7. (a) and (b) SEM micrographs showing lining–deposit interface of samples collected 12 m from the outlet of the kiln, June 2010. Arrow marks Ti depleted zone, H = hematite, C = corundum.

mm. Potassium penetrates more deeply, and in larger amounts, than sodium in the lining material, even if their oxides ($K_2O$ and $Na_2O$) are present in similar concentrations in collected deposit materials (0.1–0.2 wt%). This is in agreement with Narita et al.[14] who observed that potassium was found in concentrations five times as high in the fireclay based lining (which is comparable in composition with the chamotte based liner used in this

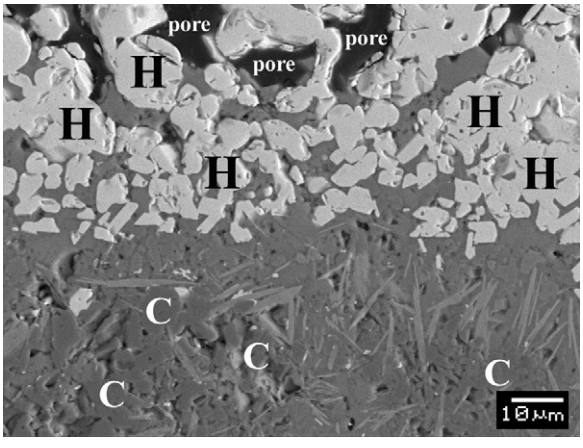


Fig. 8. SEM micrograph showing a deposit–lining interface sample, collected 30 m from the outlet of the kiln, June 2008. H = hematite, C = corundum.

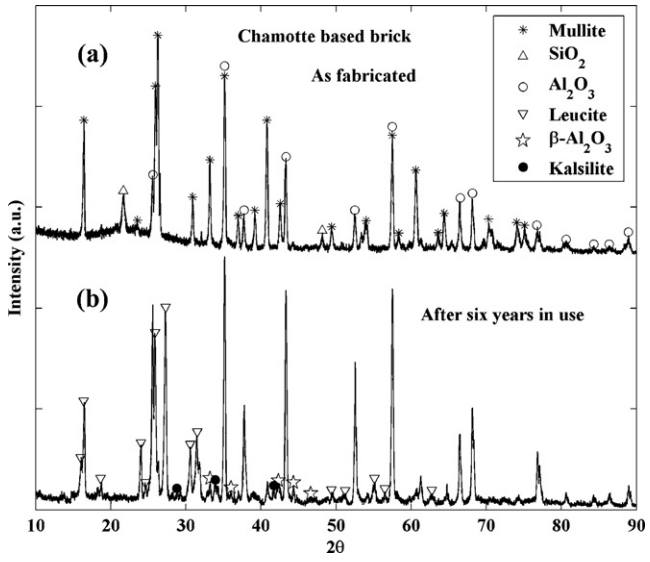


Fig. 9. (a) Diffractogram recorded on a brick sample that has served as refractory liner for 6 years in the kiln (collected 3 m from the inlet of the kiln, June 2008) and (b) diffractogram recorded on a brick sample in its fabricated condition.

study), in a blast furnace. It appears that while potassium penetrates deep into the lining and reacts with mullite and corundum, sodium acts in a more aggravating manner at the hot face, and probably forms what was observed as a glassy phase in laboratory scale studies.[7] Scudeller et al.[15] suggested that $K_2O$ starts to react with $SiO_2$, forming a glassy matrix. With time, kaliophilite ($K_2O{\cdot}Al_2O_3{\cdot}2SiO_2$), the cubic form of kalsilite, is formed. With longer times and depending on the availability of $SiO_2$, leucite ($K_2O{\cdot}Al_2O_3{\cdot}4SiO_2$) is formed, which was also formed in significant concentrations in this study.

Hematite grains remain in their original form, having sharp edges, unless they sinter. In the laboratory scale studies carried out on the same lining–deposit system with alkali metal carbonates added as corrosive agents[7,8] hematite appeared in recrystallised needle shaped formations that migrated through the lining. Alkali metals in concentrations as low as those found in the kiln do not cause melting and recrystallisation of hematite: they only promote its infiltration and sintering.

### 5.2. Penetration of iron oxide into lining

It has been observed that larger hematite grains (5–50 μm) in the deposit material remain primarily at the original lining–deposit interface. After grinding the ore, 85% of the particles are of a size below 45 μm,[16] and so the hematite particles can be assumed to be of their original size. However, some of the hematite penetrates the hot face via fissures, voids and brick joints, some forms a laminar structure with corundum from the bricks, and some migrates through the lining and grains, accumulating in clusters deeper in the lining. The driving force for the migration of hematite into the refractories is mainly capillary infiltration; where grains of hematite are in the solid state, but the infiltration is promoted by a viscous glassy phase. However, at some locations the migration mechanism of hematite could be diffusive.

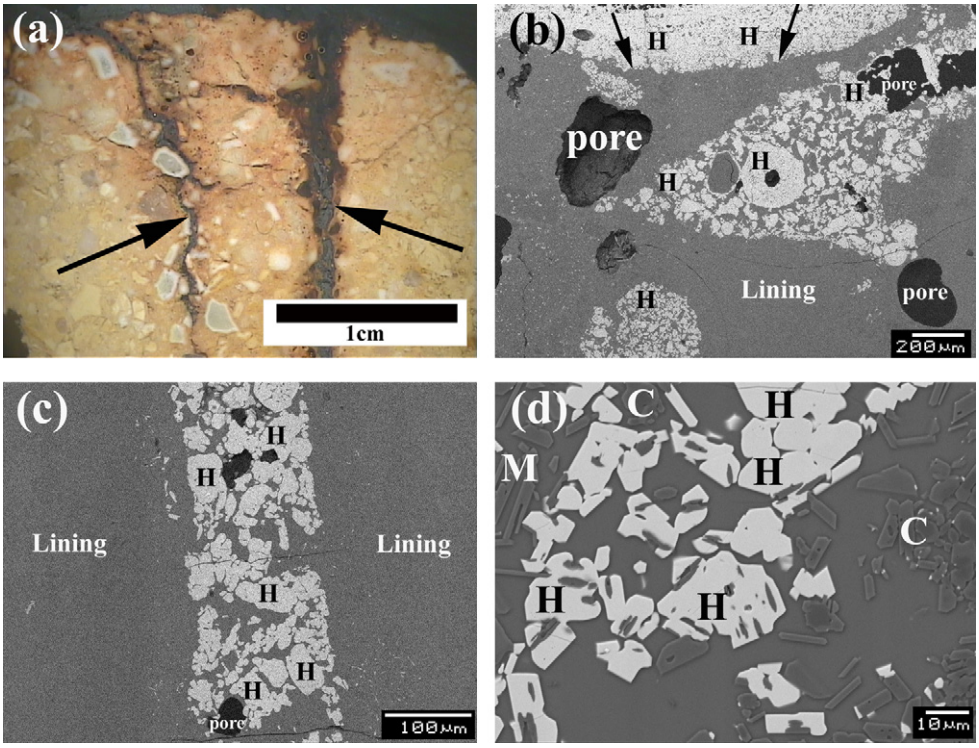


Fig. 10. (a) Optical micrograph showing a deposit–lining interface sample, where the arrow to left marks a fissure and the arrow to right marks a brick joint, (b) SEM micrograph showing deposit–lining interface where hematite has migrated into the lining, (c and d) SEM micrographs hematite filled fissures. H = hematite, C = corundum. All samples collected 25 m from the outlet of the kiln, June 2010.

The penetration of deposit material into fissures and joints acts like a glue in the brick joints, such that the bricks are sintered together and act as a monolithic lining. This is probably one of the reasons that the lining could serve as long as 8 years in one location (collected 25 m from the outlet in June 2010). Nevertheless, the zone of iron penetration is just a few mm, and the concentrations of iron containing phases were still too low to be detected by XRD analysis. However, a high concentration of cristobalite is still present, which is significant for a brick that has served as liner for 8 years at a location where fly ash falls.

### 5.3. Effect of titanium oxide on lining properties

Titanium oxide inclusions were observed in the bulk of the liner, Fig. 7(a). However, a zone ~100 μm in width closest to the deposit was depleted of these inclusions, possibly by migration through the lining towards the hematite in the deposit. Moreover, iron oxide and alumina form a laminar structure (as seen in Fig. 3(b)) where it appears that while potassium diffuses from the iron oxide into the alumina, titanium migrates from the alumina zone and diffuses into the iron oxide lamella. This might be the driving force for the formation for this laminar structure. Separation of titanium from alumina, and instead formation of a solid solution between titanium and iron oxide, is in agreement with previous work.[8] One reason for this is that corundum does not dissolve titanium in its lattice.[17] The separation of titanium oxide from alumina rich regions in the lining, by migration and diffusion, contributes to an increased exchange of material between lining and deposit.

### 5.4. Effect of variable conditions on lining properties

Degradation occurs by different mechanisms at different locations in the kiln. The outlet of the kiln, where the high alumina bricks serve as liner, is exposed to higher temperatures, whereas the inlet of the kiln, containing a chamotte based liner, is exposed to higher alkali concentrations, resulting from the fly ash from the burner. In addition, the chemical composition of the as-fabricated liners varies slightly over time from the producer. This results in different concentrations of phases forming in the two lining material samples collected. It is also observed that the concentrations of different phases and elements in the bricks, and the degradation mechanisms, vary with time on the scale of years, as expected with heterogeneous materials such as refractories.

Even at locations close to each other with similar bricks, large variations in the degradation process are observed. The sample collected 30 m from the outlet (in June 2008) had a high concentration of feldspathoid minerals, whereas no feldspathoids were detected in the lining in the sample collected 25 m from the outlet 2 years later (in June 2010), even though they were of the same quality and installed on the same occasion (in 2002). XRD reveals that alkali reacts primarily with mullite, forming feldspathoids, and secondarily with $Al_2O_3$, forming $\beta$-$Al_2O_3$ which is expected based on previous observations.[18] Corundum grains remain more intact than mullite grains, but the

grain boundaries corrode and the grains migrate into the deposit material. However, liners with grains embedded in a smaller amount of glassy bonding phase and which have a higher grain-to-grain contact area (corundum grains, Figs. 3(a) and 7(b)) are not able to resist penetration of hematite grains in the brick bulk, as well as liners with more glassy bonding phase present between the grains (corundum grains, Fig. 7(a)).

In bauxite based brick collected in the kiln in June 2010, considerable amounts of andalusite were present. Previous studies of heat treated andalusite[19] showed that grains with sizes around 5 μm transform completely to mullite within 25 h of a heat treatment at 1350 °C. For larger grains (1500 μm) 60% of the andalusite transforms to mullite within 100 h at 1350 °C. This indicates that the temperature at the hot face of the lining at these locations was considerably lower than 1350 °C.

Cracking, which can cause spall offs, is observed parallel to the hot face – in some samples through the deposit material, and in others through the lining. However, exfoliation during fall out may also continue through the lining material because of the strong bonding between deposit and lining. Therefore it is impossible to ascertain how long analysed liner samples had been exposed in the hot face. Thick accumulations of deposit that form rapidly at the surface of the lining at some locations in the kiln may act as protective thermal insulators and as protection against alkali from the fly-ash, but they also create mechanical strains. A fall out of such deposit quickly enhances the temperature of the lining at the new hot face, which may cause thermal shock and spallation.

### 5.5. Summary

The development of degradation mechanisms can here, and in general, roughly be described by: penetration of the lining by slags, alkalis or molten metals (wetting followed by capillary infiltration); corrosion (breaking of chemical bonds); and finally erosion (dislodgement of particles – depletion). Similar descriptions are reported in secondary steelmaking,[20] a lime regenerating furnace,[21] a blast furnace,[14] copper production,[22] and during the production of stainless steel.[23]

We propose that vaporised potassium penetrates voids, fissures and brick joints, where it is entrapped by liquids, condenses and diffuses through the bulk, reacting with the lining material and nucleating in the brick bulk primarily as feldspathioid minerals, and also as β-$Al_2O_3$. This is enhanced by sodium, which lowers eutectic temperatures. Hematite from the deposit material starts to react with corundum from the brick. One of the driving forces for this is the exchange of titanium. The brick degradation is caused by concurrently active processes of chemical reactions and migration of grains from the refractory lining into the deposit material and vice versa.

## 6. Conclusions

- Potassium penetrates the surface of liner bricks in much higher concentration than sodium, to a depth of several mm.
- The presence of potassium causes the formation of secondary mullite around the aggregates of primary mullite, which is a corrosive mechanism that promotes degradation of the lining.
- Phases such as kalsilite, leucite and potassium β-alumina are formed, as a consequence of potassium migration, which contribute to the degradation of the lining.
- Grains of hematite with sizes between 5 and 50 μm remain primarily at the original interface between the lining and deposit material.
- Some hematite penetrates fissures/cracks, voids and brick joints, some forms a laminar structure with corundum from the bricks, and some migrates in grains, or clustered grains through the lining material.
- Exchange of titanium oxide from the lining into the deposit material is one of the driving forces that creates a larger contact area between lining and deposit at the hot face, affecting degradation.
- Degradation is non-uniform along the kiln, although the trends above are observed.
- Degradation is caused by simultaneous chemical reactions, finally resulting in the migration of eroded grains from the lining into the deposit material.

## Acknowledgements

The authors are grateful to LKAB for help with chemical analysis, and to Knut Lindmark, SÅAB (Svappavaara Åkeri Limited), for collection of samples. One author, J.S., is also grateful for financial support from Hjalmar Lundbohm Research Centre (HLRC).

## References

1. Zhang Y, Feng J, Xu J, Zhang Y, Yang J. Energy and exergy analyses of a mixed fuel-fired grate-kiln for iron ore pellet induration. *Energy Convers Manage* 2011;**52**(5):2064–71.
2. Jiang T, He G-Q, Gan M, Li G-H, Fan X-H, Yuan L-S. Forming mechanisms of rings in rotary-kiln for oxidized pellet. In: *Proceedings of the 5th international congress on the science and technology of ironmaking*. 2009. p. 292–7.
3. Uenaka T, Isako H, Tokutake K, Aketa K. Coal firing in pelletizing plant developed by Kobe Steel. *Ironmaking Steel Making* 1983;**10**(5):234–9.
4. Ko Y-C. Wear of refractories in the iron and steel industry. *SEAISI Quart* 1991;**20**(2):19–29.
5. Schneider H, Schreuer J, Hildman B. Structure and properties of mullite – a review. *J Eur Ceram Soc* 2008;**28**(2):329–44.
6. DeLucia M, Wolfe H. Refractories to contain fluorinated waste streams. *Waste Manage* 2000;**20**(5):449–54.
7. Stjernberg J, Antti M-L, Nordin L-O, Odén M. Degradation of refractory bricks used as thermal insulation in rotary kilns for iron ore pellets production. *Appl Ceram Technol* 2009;**6**(6):717–26.
8. Stjernberg J, Lindblom B, Wikström J, Antti M-L, Odén M. Microstructural characterization of alkali metal mediated high temperature reactions in mullite based refractories. *Ceram Int* 2010;**36**(2):733–40.
9. Pownceby M, Constanti-Carey K, Fisher-White M. Subsolidus phase relationships in the system $Fe_2O_3$–$Al_2O_3$–$TiO_2$ between 1000° and 1300 °C. *J Am Ceram Soc* 2004;**86**(6):975–80.
10. Iqbal Y, Lee W. Fired porcelain microstructures revisited. *J Am Ceram Soc* 1999;**82**(12):3584–90.
11. Iqbal Y, Lee W. Microstructural evolution in triaxial porcelain. *J Am Ceram Soc* 2000;**83**(12):3121–7.

12. Lee W, Iqbal Y. Influence of mixing on mullite formation in porcelain. *J Eur Ceram Soc* 2001;**21**(14):2583–6.
13. Schüller K. Reactions between mullite and glassy phase in porcelains. *Trans Br Ceram Soc* 1964;**64**(2):103–17.
14. Narita K, Onoye T, Satoh Y, Miyamoto M, Taniguchi K, Kamatani S, et al. Effects of alkalis and zinc on the wear of blast furnace refractories. *ISIJ* 1981;**21**(12):839–45.
15. Scudeller L, Longo E, Varela J. Potassium vapor attack in refractories of the alumina-silica system. *J Am Ceram Soc* 1990;**73**(5):1413–6.
16. Forsmo SPE. Oxidation of magnetite concentrate powders during storage and drying. *Int J Miner Process* 2005;**75**(1–2):135–44.
17. Das K, Choudhury P, Das S. The Al─O─Ti (aluminum–oxygen–titanium) system. *J Phase Equilib* 2002;**23**(6):525–35.
18. Farris R, Allen J. Aluminous refractories – alkali reactions. *Iron Steel Eng* 1973;**50**(2):67–74.
19. Bouchetoua M-L, Ildefonse J-P, Poirier J, Daniellou P. Mullite grown from fired andalusite grains: the role of impurities and of the high temperature liquid phase on the kinetics of mullitization and consequences on thermal shocks resistance. *Ceram Int* 2005;**31**(7):999–1005.
20. Ishii A, Goto K. Wear of refractories in secondary steelmaking. *Taikabutsu Overseas* 1993;**13**(4):30–5.
21. Malyshev IP, Troyan VD, Troshenkov NA, Pribora VN, Likhodievskii AV, Pyrikov AN, et al. MLS-62 refractories in lining lime-regenerating rotating ovens. *Refract Ind Ceram* 2007;**48**(1):12–6.
22. Petkov V, Jones PT, Boydens E, Blanpain B, Wollants P. Chemical corrosion mechanisms of magnesia–chromite and chrome-free refractory bricks by copper metal and anode slag. *J Eur Ceram Soc* 2007;**27**(6):2433–44.
23. Van Ende MA, Guo M, Jones PT, Blanpain B, Wollants P. Degradation of MgO─C refractories by MnO-rich stainless steel slags. *Ceram Int* 2009;**35**(6):2203–12.